The Astrophysical Journal Letters, 761:L23 (5pp), 2012 December 20 doi:10.1088/2041-8205/761/2/L23

FAILED-DETONATION SUPERNOVAE: SUBLUMINOUS LOW-VELOCITY Ia SUPERNOVAE AND THEIR KICKED REMNANT WHITE DWARFS WITH IRON-RICH CORES

George C. Jordan IV[1,2], Hagai B. Perets[3,4], Robert T. Fisher[5], and Daniel R. van Rossum[1,2]
[1] Center for Astrophysical Thermonuclear Flashes, The University of Chicago, Chicago, IL 60637, USA
[2] Department of Astronomy and Astrophysics, The University of Chicago, Chicago, IL 60637, USA
[3] Physics Department, Technion, Israel Institute of Technology, Haifa 32000, Israel
[4] Harvard-Smithsonian Center for Astrophysics, 60 Garden St., Cambridge, MA 02138, USA
[5] Department of Physics, University of Massachusetts Dartmouth, 285 Old Westport Road, North Dartmouth, MA 02740, USA
Received 2012 August 24; accepted 2012 November 12; published 2012 December 3

ABSTRACT

Type Ia supernovae (SNe Ia) originate from the thermonuclear explosions of carbon–oxygen (C–O) white dwarfs (WDs). The single-degenerate scenario is a well-explored model of SNe Ia where unstable thermonuclear burning initiates in an accreting, Chandrasekhar-mass WD and forms an advancing flame. By several proposed physical processes, the rising, burning material triggers a detonation, which subsequently consumes and unbinds the WD. However, if a detonation is not triggered and the deflagration is too weak to unbind the star, a completely different scenario unfolds. We explore the failure of the gravitationally confined detonation mechanism of SNe Ia, and demonstrate through two-dimensional and three-dimensional simulations the properties of failed-detonation SNe. We show that failed-detonation SNe expel a few 0.1 $M_{\odot}$ of burned and partially burned material and that a fraction of the material falls back onto the WD, polluting the remnant WD with intermediate-mass and iron-group elements that likely segregate to the core forming a WD whose core is iron rich. The remaining material is asymmetrically ejected at velocities comparable to the escape velocity from the WD, and in response, the WD is kicked to velocities of a few hundred km s^{-1}. These kicks may unbind the binary and eject a runaway/hypervelocity WD. Although the energy and ejected mass of the failed-detonation SN are a fraction of typical thermonuclear SNe, they are likely to appear as subluminous low-velocity SNe Ia. Such failed detonations might therefore explain or are related to the observed branch of peculiar SNe Ia, such as the family of low-velocity subluminous SNe (SN 2002cx/SN 2008ha-like SNe).

Key words: hydrodynamics – ISM: supernova remnants – supernovae: general – supernovae: individual (2002cx, 2008ha) – white dwarfs

1. INTRODUCTION

Type Ia supernovae (SNe Ia) are among the most energetic explosions in the known universe, releasing $\sim 10^{51}$ erg of kinetic energy in their ejecta, and synthesizing $\sim 0.7\ M_{\odot}$ of radioactive ^{56}Ni. The discovery of the Phillips relation (Pskovskii 1977; Phillips 1993) enabled the use of SNe Ia as standardizable cosmological candles, and has ushered in a new era of astronomy leading to the discovery of the acceleration of the universe (Riess et al. 1998; Schmidt et al. 1998; Perlmutter et al. 1999) and to the 2011 Nobel Prize in physics.

Models of normal SNe Ia, such as the single-degenerate (SD) model, focus on exploding the WD in order to produce the explosion energies, luminosities, and typical velocities observed in normal SNe Ia. This is accomplished either by consuming enough of the WD with the initial subsonic burning phase—or deflagration phase—to unbind the WD as theorized by the pure deflagration (PD) model (Gamezo et al. 2005; Röpke & Hillebrandt 2005), or by consuming the entire WD by a detonation triggered by the deflagration phase as posited by the deflagration-to-detonation transition (DDT; Khokhlov 1991; Gamezo et al. 2004, 2005), the pulsating reverse detonation (PRD; Bravo & García-Senz 2009; Bravo et al. 2009), and the gravitationally confined detonation (GCD; Calder et al. 2004; Jordan et al. 2008, 2012; Meakin et al. 2009) models of SNe Ia.

In the following, we present a novel variant of SD model of SNe Ia in which the deflagration is too weak to unbind the star[6] and a detonation is not triggered by any of the proposed mechanisms, resulting in the survival of a bound remnant of the original WD. We present for the first time predictions of these failed-detonation (FD) SNe from two-dimensional (2D) and 3D simulations. We show that FD models have numerous remarkable implications for the observable properties of the resulting explosion and its outcomes. These include the production of a family of peculiar SNe Ia events with low expansion velocities, low luminosities, and low ejecta mass—whose properties are broadly consistent with the observed properties of a branch of peculiar SNe Ia similar to SN 2002cx and/or SN 2008ha. Even more remarkably, the remnant WD receives a large velocity kick from the asymmetric nature of the deflagration, and is enriched with both intermediate-mass elements (IMEs) and iron-group elements (IGEs), forming a peculiar WD with a heavy/iron-rich core.

Previous work has suggested that though the PD model has shortcomings explaining normal SNe Ia, they may explain 2002cx-like SNe (Branch et al. 2004). The WD, however, is fully incinerated in these models, producing a Chandrasekhar mass of ejecta. Such models might therefore not be able to explain the large diversity recently observed among SNe of this peculiar class of SNe. Additionally, a study by Livne et al. (2005) of initial conditions for the PD model produced situations that they called "fizzles" that did not produce a healthy PD explosion and

[6] We acknowledge related work by Kromer et al. (2012) that appeared as this Letter was going to press.

Table 1
Simulations Properties

Sim. Name	Δx[a] (km)	n_{ign}[b]	r_{ign}[c] (km)	z_{ign}[d] (km)	E_{nuc}[e] (E_{bin})	C–O_B[f] ($M_\odot$)	IME_B ($M_\odot$)	IGE_B ($M_\odot$)	v_B[g] (km s^{-1})	C–O_E[h] ($M_\odot$)	IME_E ($M_\odot$)	IGE_E ($M_\odot$)	$E_{kin,E}$[i] ($\times 10^{50}$ erg)	$v_{ave,E}$[j] (km s^{-1})
2D70	4	4	64.0	70.0	0.89	0.93	0.07	0.13	119	0.13	0.03	0.07	0.32	3730
3D48	8	63	128.0	48.0	1.06	0.84	0.06	0.09	351	0.16	0.05	0.16	0.90	4932
3D38	8	63	128.0	38.0	1.30	0.68	0.05	0.05	411	0.27	0.09	0.24	1.6	5139
3D28	8	63	128.0	28.0	1.51	0.49	0.03	0.04	549	0.41	0.13	0.30	2.3	5229
3D18	8	63	128.0	18.0	1.67	0.26	0.02	0.02	483	0.58	0.17	0.34	2.9	5193

Notes.
[a] Maximum spatial resolution.
[b] Number of ignition points.
[c] Radius of the spherical volume containing the ignition points.
[d] Z coordinate of the origin of the spherical volume containing the ignition points.
[e] Energy released during the deflagration phase divided by the binding energy of the star ($E_{bin} = 4.5 \times 10^{50}$ erg).
[f] "B" refers to gravitationally bound material.
[g] Velocity of the gravitationally bound material.
[h] "E" refers to material that will escape the system.
[i] Average kinetic energy of the escaping material.
[j] Mass-weighted velocity of escaping material.

left the WD bound. They did not pursue these models beyond the scope of their study, and did not relate these fizzles to peculiar SNe Ia.

2. AVOIDING THE TRANSITION TO DETONATION

The FD scenario requires that no detonation is triggered as a result of the deflagration event. We briefly touch on the possibility of the PRD and GCD failing to trigger a detonation. We first make the general assumption that is made in the PD, PRD, and GCD scenarios, namely that the DDT mechanism is not active. We refer the reader to Bravo & García-Senz (2009) for a discussion of the justification of this assumption; the details of which are beyond the scope of this work.

In the PRD model, ash ejected during the deflagration phase falls back onto the WD. An accretion shock formed by infalling ash surrounds and heats fuel remaining in the WD core, which in turn triggers a detonation. Bravo & García-Senz (2009) reported that the PRD could not trigger a detonation if the energy released during the deflagration was near that of the binding energy of the WD. This situation is realized in our simulations.

Jordan et al. (2012, hereafter J12) detail how the GCD mechanism triggers a gradient-induced detonation when ash from the deflagration flows over the stellar surface, mixes with cold fuel, collides at the antipodal point from break out, and is squeezed to the necessary temperatures and densities by the contracting WD. Models presented here show that a detonation via the GCD mechanism is avoided altogether. The primary difference between these models and those of J12 is the amount of energy released during the deflagration. More energy is released and delivered to the WD than in J12; thus, more mass is consumed by the flame and ejected from the WD than previously. The WD is modified to a higher degree and as a result the WD cannot contract enough to squeeze the fuel–ash mixture to the critical conditions for detonation. Therefore the star never detonates. We note that Röpke et al. (2007) also investigated the failure of the GCD mechanism; however, their simulations in which the WD was still bound and star did not detonate were stopped before the contraction phase. J12 discussed these models and showed that had Röpke et al. (2007) run their simulations longer, they would have most likely triggered a GCD on contraction.

The FD scenario thus occurs when a weak deflagration leaves a partially bound WD (in contrast to the PD model) and the conditions for detonation are never realized (and the DDT is avoided).

3. SIMULATIONS OF THE FD MODEL

3.1. Simulation Setup

We used the adaptive mesh refinement FLASH application framework (Dubey et al. 2009; Fryxell et al. 2000) to perform our simulations of FD models. FLASH has been previously used to simulate SNe Ia in both 2D cylindrical and 3D Cartesian geometry (Jordan et al. 2008; Meakin et al. 2009; Krueger et al. 2012; J12). Our simulations include an advection–diffusion–reaction treatment of the thermonuclear flame (Calder et al. 2007; Townsley et al. 2007; Seitenzahl et al. 2009), an equation of state that includes contributions from blackbody radiation, ions, and electrons of an arbitrary degree of degeneracy (Timmes & Swesty 2000), and the multipole treatment of gravity (ASC FLASH Center 2012).

We performed four 3D exploratory simulations to test the feasibility of the FD and one full 2D model to adequately observe the FD at late times.

Our 3D simulations included a reduced domain size and a moderate resolution (8 km) which reduced their computational expense. We initialized these simulations similarly to those in J12 with a 1.365 $M_\odot$ WD placed at the origin of the domain. We used the same distribution of 63 16 km radius ignition "points" distributed in a 128 km radius spherical volume. We chose 48 km, 38, km, 28 km, and 18 km as offset distances along the z-axis of the spherical volume. Note that these offsets are closer to the WD core than in J12 and lead to more burning during the deflagration phase. Table 1 lists the initial conditions for each simulation and the corresponding names we gave them. We ran the simulations from ignition through peak stellar expansion, and at least until the WD reached a maximum central density upon contraction.

Our 2D simulation was performed with a large domain in 2D cylindrical geometry at 4 km resolution and ran for 60 s. This simulation was initialized similarly to the 3D simulations, except we placed only four bubbles in a 64 km spherical volume offset by 70 km along the z-axis (axis of symmetry). We chose

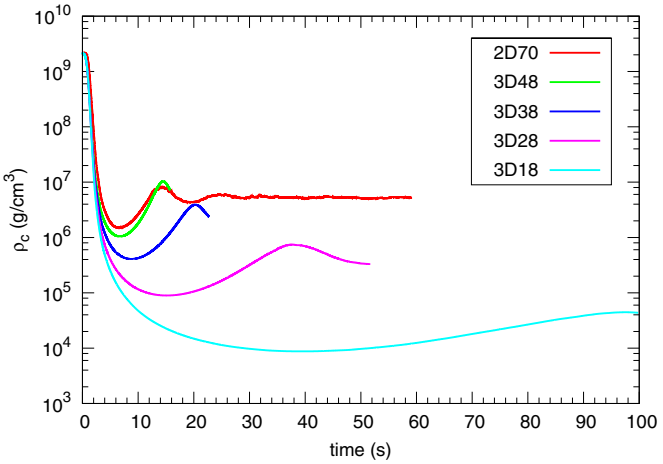

Figure 1. Central density, ρ_c, of the WD vs. time.

these initial conditions to obtain an FD in 2D given what we learned from our 3D simulations. The larger domain size allowed us to follow the outer layers of the ejecta for the entirety of the simulation.

3.2. Simulation Results

We obtained an FD from each of our simulations. Table 1 contains a collection of their properties.

The deflagration liberated between 89% and 167% of the binding energy of the WD. However, in each simulation the deflagration fails to unbind the WD. The WD expands in response to the deflagration, reaches its maximum level of expansion, and then contracts. Figure 1 shows the evolution of the central density, ρ_c, of the WD and illustrates the oscillatory nature of the WD after the deflagration. The more energy released during the deflagration, the more the star expanded, the longer the pulsational period, and the smaller ρ_c at maximum contraction.

The fact that the deflagration releases more than 100% WD binding energy in some models suggests that the WD should be unbound after the deflagration; however, the entire energy budget does not work to only unbind the star. For example, some of the energy is lost when the ejecta and the remnant WD are accelerated to high velocities. Even though the deflagration liberates enough energy to completely unbind the star, the energy is partitioned in such a way that a portion of the original WD remains gravitationally bound.

In each of our models, the WD gets a kick in the opposite direction from which the buoyant ash rises and breaks through the surface of the star. We measured this velocity to be on the order of hundreds of km $s^{-1}$and list these values for each simulation in Table 1. We note that momentum conservation is better than 10% of the momentum of the WD kick in our simulations. Some of the material from the FD escapes and achieves high velocities, while some of the material is bound to the remnant WD and will eventually accrete onto its surface. Table 1 lists the composition of material that remains gravitationally bound and eventually will mix with the remnant WD. In all cases, between 0.04 $M_\odot$ and 0.2 $M_\odot$ of IMEs and IGEs (some of which are radioactive ^{56}Ni) remained bound to the star. The evolution of the WD as the material falls back onto and heats the star is an interesting question and one which we will examine in future work.

The composition of the material that escapes the system is also listed in Table 1 along with the kinetic energy and the mass-weighted velocity of the ejecta. This material includes carbon and oxygen, IMEs, and IGEs, and ranges from 0.2 $M_\odot$ to 1.0 $M_\odot$. In general, the more material that is burned during the deflagration, the more material that escapes.

Figure 2 shows the density structure and composition with overlaid velocity contours of the 2D model at 60 s. Note that the density profile of the FD model is asymmetric in velocity space between the hemisphere corresponding to the ejected deflagration and the opposite hemisphere of the system. The remnant of the WD can be seen as the tiny high-density feature slightly below the origin of the domain.

The figure also shows the nature of the asymmetry in composition of the structure. The north side of the remnant contains the products of the deflagration that were sprayed from the surface of the WD. Clumpy structures of IMEs and IGEs exist at a range of velocities in the northern hemisphere of the domain but are less abundant in the southern hemisphere. The asymmetries suggest that this object would look much different depending on the viewing angle of the observer.

All of our models produce a relatively small amount of radioactive ^{56}Ni. Although we do not perform detailed nucleosynthetic post-processing of the 3D models, we can set an upper limit on the ^{56}Ni yields with the amount of IGEs produced, which ranges from 0.2 $M_\odot$ to 0.34 $M_\odot$. Neutronization through electron capture reactions during the deflagration would shift production away from ^{56}Ni though and reduce its contribution to the IGE totals. Whether even lower masses of IGEs (and thus ^{56}Ni) could be produced under appropriate conditions (e.g., comparable to that observed in SN 2008ha, a very faint SN with extremely low ejecta velocities) is yet to be explored.

In summary, we find that a remnant of the WD survives the FD SN event with a lower mass than the original. The remaining bound stellar material is kicked by the ejection of the ash and obtains a velocity of hundreds of km s^{-1}. An asymmetric outburst of deflagration products rich in IGEs (such as Fe, Co, and Ni) and containing some IMEs (such as Mg, Si, and S) is produced. Some of this material attains escape velocity and some falls back onto the star. The velocity of the escaping outflow was slow (approximately a few thousand km s^{-1}) related to normal SNe Ia as a result of the comparatively small amount of energy released in the FD scenario. Due to the weak nature of the deflagration, the FD only converted 15% and 25% of the WD to ^{56}Ni, compared to normal SNe Ia which convert nearly half of the WD to ^{56}Ni.

4. DISCUSSION AND PREDICTIONS

4.1. Subluminous Low-velocity SNe

The most prominent features of the FD models are the low mass and low velocity of the ejecta, which translate into the production of typically subluminous, low-velocity SNe Ia. It is therefore natural to examine whether SNe with such characteristics have already been discovered. In particular, one may explore peculiar SNe exhibiting either extremely low mass ejecta, such as SN 2008ha (Foley et al. 2009; Valenti et al. 2009), or low ejecta velocity such as SN 2002cx-like SNe (Li et al. 2003; Branch et al. 2004; Jha et al. 2006).

Normal SNe Ia differ in their ejecta velocities as measured in some standard method, but they generally fall between 9000 km s^{-1} and 14,000 km s^{-1} near peak luminosity, with similar dispersion at later times (as derived from the Si II line; Benetti et al. 2005). The velocities of even the lowest velocity SNe in the Benetti et al. (2005) sample much exceed

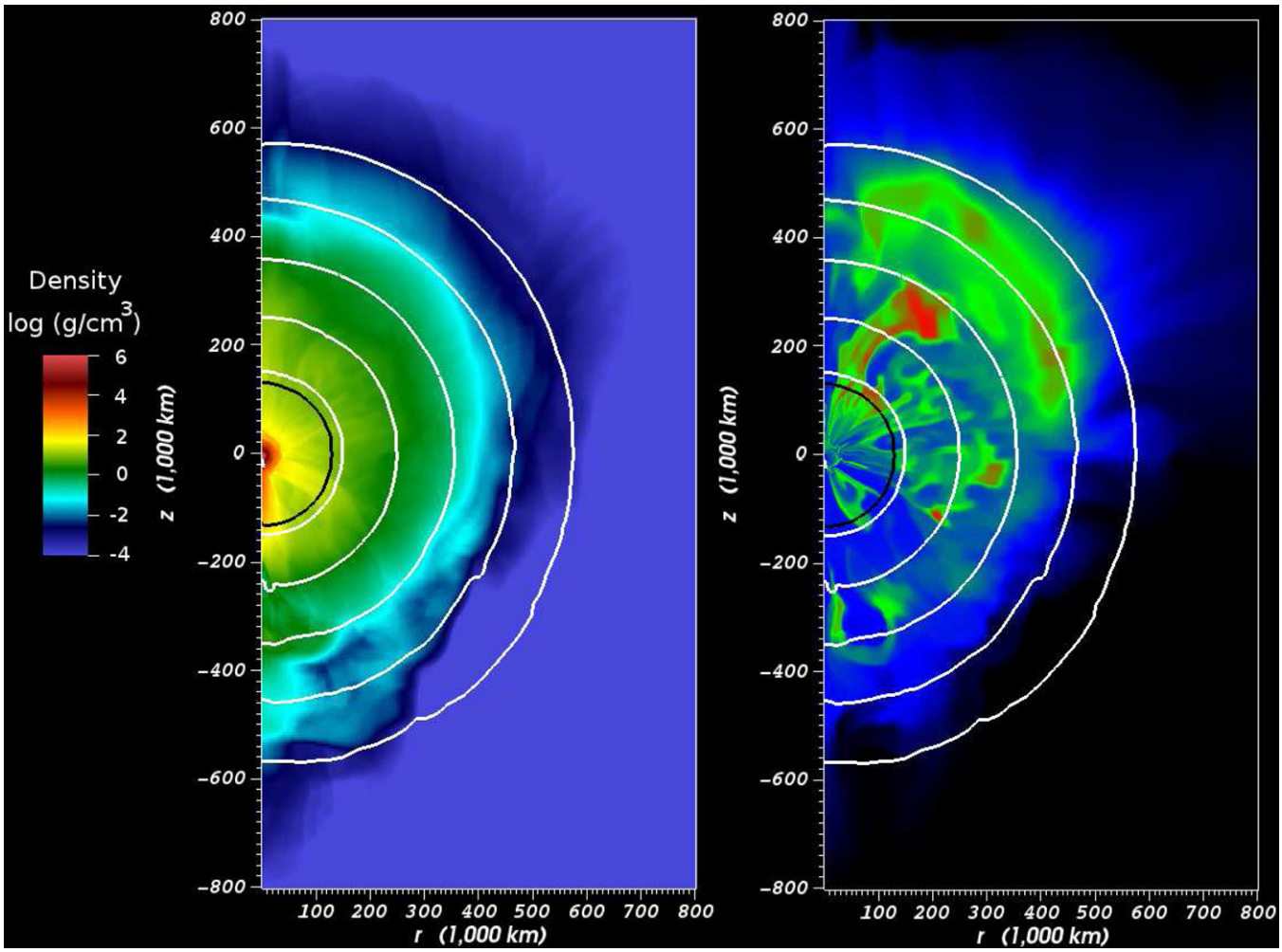

Figure 2. Images from the 2D70 simulation. The black contour marks the transition between gravitationally bound and escaping material. The white contours are of the magnitude of the velocity field. From the innermost contour and moving outward, the values are 2000 km s^{-1}, 4000 km s^{-1}, 6000 km s^{-1}, 8000 km s^{-1}, and 10,000 km s^{-1}. The images show the simulation at 60 s. Left: log density of the remnant. The values of the density are given by the color bar on the left. Right: the composition of the remnant. Blue is C–O, green is IMEs, and red is IGEs.

the mass-averaged FD velocities listed in Table 1. We also note a trend in our simulations of more energetic and likely more luminous (larger IGE yield) SNe to be accompanied by higher ejecta velocities over almost an order of magnitude in kinetic energy. The only other type of SNe with such low expansion velocities is the branch of peculiar SNe Ia, named for the prototype for this class of supernovae, 2002cx (Li et al. 2003; Branch et al. 2004; Jha et al. 2006); such SNe may also have an energy–velocity correlation (McClelland et al. 2010) as observed in our simulations.

SN-2002cx-like events are characterized by luminosities that lie too low in comparison to the Phillips relation for Branch-normal Ia events (Li et al. 2003), low photospheric velocities (Li et al. 2003), weak IME lines (Branch et al. 2004), and late-time optical nebular spectra dominated by narrow Fe II lines (Branch et al. 2004; Jha et al. 2006). Since the discovery of SN 2002cx, a number of other 2002cx-like events have been discovered, including 2002es, 2005P, 2005hk (Chornock et al. 2006), 2008ge (Foley et al. 2010a), and 2008ha (Foley et al. 2009; Valenti et al. 2009). The latter event (SN 2008ha), in particular, is consistent with extremely low mass ejecta and energetics. We predict the FD models to produce similar properties to those characterizing SN 2002cx-like SNe, given the low expansion velocities and the low estimated ^{56}Ni yield, and potentially even explaining SN 2008ha-like events with low-mass ejecta.

Though our initial set of simulations is limited, the robust features of FDs, including low-velocity ejecta, the expected low luminosity (due to the small yield of ^{56}Ni) and their low-mass ejecta (comparable to that SN 2008ha) make them tantalizing candidate progenitors for this branch of peculiar SNe. Note that the SD origin of such SNe is also consistent with the overall typically young (but not *necessarily* young; Foley et al. 2010b) environments found for SN 2002cx-like SNe, compared to the expectations from, e.g., core-collapse SNe (only very young environments).

4.2. WDs with Heavy/Iron-rich Cores

In our FD scenario, a large amount of burnt material falls back to the remnant WD. From Table 1, the WD may incorporate as much as 0.3 $M_\odot$ of IGEs and 0.07 $M_\odot$ of IMEs of fallback material, together comprising as much as ∼18% of the remnant C–O WD. In time, these elements are likely to gravitationally settle to the WD core, creating WDs with iron-rich/heavy core. The existence of iron-core WDs has been considered before, with even the potential observation of such WDs (Provencal et al. 1998; Catalán et al. 2008). The FD scenario therefore provides a novel evolutionary scenario for the formation of

these iron/heavy-core C–O WDs. A somewhat related scenario of failed SN was suggested for the formation of O–Ne–Mg WDs with iron cores (Isern et al. 1991).

4.3. WD Natal Kicks

FDs produce a highly asymmetric ejection of material. This is not unique amongst various models for SNe explosions. However, in our FD case, the WD survives the explosion. Considering momentum conservation, this gives rise to a unique outcome, namely that the surviving WD is kicked at very high velocities, ranging hundreds of km s^{-1}. The FD scenario suggests the existence of strong WD natal kicks, and provides an interesting prediction per the existence of hypervelocity WDs. Taken together, the potential existence of a heavy core WD (discussed in Section 4.2) and the high ejection velocity produce a highly peculiar object, which, if observed, may provide a possibly unique smoking gun signature. One should note, however, that the population of halo WDs may also have relatively high velocities, and it might therefore be difficult to pinpoint the kinematic property as related to a natal kick (unless the WD is massive and young; an unlikely possibility for the old population of halo WDs).

We note that velocities of hundreds of km s^{-1} could be larger than the orbital velocities of the SN binary progenitor, and a kick velocity of such magnitude can therefore unbind the binary. Various binary configurations have been explored for the SD progenitor models, including progenitors with Main Sequence (MS) and Red Giant (RG) companions (Hachisu et al. 1996; Marietta et al. 2000). We conclude that the range of WD kick velocities could either unbind the binary (more likely for WD–MS binaries) or leave behind a bound WD binary (more likely for the WD–RG binaries). The latter case could lead to the formation of a very compact, but potentially eccentric WD binary, which would be difficult to produce through other channels of binary evolution.

5. SUMMARY

Our simulations demonstrate the properties of a scenario in which the deflagration is too weak to unbind the WD and the conditions to trigger a detonation are not met. These FDs result in an asymmetric outburst of deflagration material consisting of IMEs and IGEs along with a fraction of the original WD still gravitationally bound. The models produce a family of faint SNe Ia with a slowly evolving light curves due to the low ^{56}Ni yield and the low energetics. The remaining WD gets a kick on the order of hundreds of km s^{-1} and is contaminated with fallback from the deflagration, producing a WD with an iron-rich/heavy core. We presented our initial simulations to quantify the some of the bulk observable properties and demonstrate the conditions under which the GCD fails. We further hypothesize that the FD model is a possible explanation for 2002cx-like SN. Future studies will explore the detailed observational features of FD SNe and their direct comparison to observations.

The authors thank the FLASH Code Group, the FLASH Astrophysics Group, and the Argonne Leadership Computing Facility at Argonne National Laboratory. H.B.P. is supported by the CfA and BIKURA prize fellowships. This work was supported in part at the University of Chicago by the US Department of Energy (DOE) under contract B523820 to the ASC Alliances Center for Astrophysical Nuclear Flashes, and in part by the National Science Foundation under grant No. AST-0909132 for the "Petascale Computing of Thermonuclear Supernova Explosions." This research used computational resources awarded under the INCITE program at ALCF at ANL, which is supported by the Office of Science of the US Department of Energy under contract no. DE-AC02-06CH11357.

REFERENCES

ASC FLASH Center 2012, FLASH User's Guide (4th ed.; Chicago, IL: Univ. Chicago), http://flash.uchicago.edu/website/codesupport/flash4_ug/
Benetti, S., Cappellaro, E., Mazzali, P. A., et al. 2005, ApJ, 623, 1011
Branch, D., Baron, E., Thomas, R. C., et al. 2004, PASP, 116, 903
Bravo, E., & García-Senz, D. 2009, ApJ, 695, 1244
Bravo, E., García-Senz, D., Cabezón, R. M., & Domínguez, I. 2009, ApJ, 695, 1257
Calder, A. C., Plewa, T., Vladimirova, N., Lamb, D. Q., & Truran, J. W. 2004, arXiv:astro-ph/0405162
Calder, A. C., Townsley, D. M., Seitenzahl, I. R., et al. 2007, ApJ, 656, 313
Catalán, S., Ribas, I., Isern, J., & García-Berro, E. 2008, A&A, 477, 901
Chornock, R., Filippenko, A. V., Branch, D., et al. 2006, PASP, 118, 722
Dubey, A., Antypas, K., Ganapathy, M., et al. 2009, Parallel Comput., 35, 512
Foley, R. J., Chornock, R., Filippenko, A. V., et al. 2009, AJ, 138, 376
Foley, R. J., Rest, A., Stritzinger, M., et al. 2010a, AJ, 140, 1321
Foley, R. J., Rest, A., Stritzinger, M., et al. 2010b, AJ, 140, 1321
Fryxell, B., Olson, K., Ricker, P., et al. 2000, ApJS, 131, 273
Gamezo, V. N., Khokhlov, A. M., & Oran, E. S. 2004, Phys. Rev. Lett., 92, 211102
Gamezo, V. N., Khokhlov, A. M., & Oran, E. S. 2005, ApJ, 623, 337
Hachisu, I., Kato, M., & Nomoto, K. 1996, ApJ, 470, L97
Isern, J., Canal, R., & Labay, J. 1991, ApJ, 372, L83
Jha, S., Branch, D., Chornock, R., et al. 2006, AJ, 132, 189
Jordan, G. C., IV, Fisher, R. T., Townsley, D. M., et al. 2008, ApJ, 681, 1448
Jordan, G. C., IV, Graziani, C., Fisher, R. T., et al. 2012, ApJ, 759, 53
Khokhlov, A. M. 1991, A&A, 245, 114
Kromer, M., Fink, M., Stanishev, V., et al. 2012, arXiv:1210.5243
Krueger, B. K., Jackson, A. P., Calder, A. C., et al. 2012, ApJ, 757, 175
Li, W., Filippenko, A. V., Chornock, R., et al. 2003, PASP, 115, 453
Livne, E., Asida, S. M., & Höflich, P. 2005, ApJ, 632, 443
Marietta, E., Burrows, A., & Fryxell, B. 2000, ApJS, 128, 615
McClelland, C. M., Garnavich, P. M., Galbany, L., et al. 2010, ApJ, 720, 704
Meakin, C. A., Seitenzahl, I., Townsley, D., et al. 2009, ApJ, 693, 1188
Perlmutter, S., Aldering, G., Goldhaber, G., et al. 1999, ApJ, 517, 565
Phillips, M. M. 1993, ApJ, 413, L105
Provencal, J. L., Shipman, H. L., Hog, E., & Thejll, P. 1998, ApJ, 494, 759
Pskovskii, I. P. 1977, SvA, 21, 675
Riess, A. G., Filippenko, A. V., Challis, P., et al. 1998, AJ, 116, 1009
Röpke, F. K., & Hillebrandt, W. 2005, A&A, 431, 635
Röpke, F. K., Woosley, S. E., & Hillebrandt, W. 2007, ApJ, 660, 1344
Schmidt, B. P., Suntzeff, N. B., Phillips, M. M., et al. 1998, ApJ, 507, 46
Seitenzahl, I. R., Townsley, D. M., Peng, F., & Truran, J. W. 2009, At. Data Nucl. Data Tables, 95, 96
Timmes, F. X., & Swesty, F. D. 2000, ApJS, 126, 501
Townsley, D. M., Calder, A. C., Asida, S. M., et al. 2007, ApJ, 668, 1118
Valenti, S., Pastorello, A., Cappellaro, E., et al. 2009, Nature, 459, 674